International Conference on Renewable Energies and Power Quality (ICREPQ'14)
Cordoba (Spain), 8th to 10th April, 2014
Renewable Energy and Power Quality Journal (RE&PQJ)
ISSN 2172-038 X, No.12, April 2014

Blade shape influence on aerodynamic efficiency of a Magnus wind turbine using particle image velocimetry

A. Massaguer[1], E. Massaguer[1], T. Pujol[1], M. Comamala[1], and J. Velayos[1]

[1] Department of Mechanical Engineering and Industrial Construction
Polytechnic High School, University of Girona
Campus de Montilivi, 17071 Girona (Spain)
Phone/Fax number:+0034 972 419654, e-mail: **albert.massaguer@udg.edu**

Abstract. Magnus wind turbine uses rotating cylinders instead of conventional horizontal axis blades. These cylinders rotate around their own axes and create a rotational force according to Magnus effect. Although this kind of wind turbines have many benefits over conventional axis blades and can exhibit different blade characteristics, it is not clearly demonstrated which the most efficient blade geometry is. This paper focuses on assess the influence of the blade shape on the Mangus force, using particle image velocimetry.

Key words

Magnus wind turbine, renewable energy, blade geometry, wind energy, particle image velocimetry.

1. Introduction

Wind power plays a key role in addressing climate change. Developing wind power and other clean sources reduces the use of fossil fuels, reduces carbon dioxide emissions and helps to stabilize our climate.

It is one of the cheapest and most abundant sources of renewable energy. On the other hand, the energy density is small, since the power generated is dependent on the size of the turbine, the wind direction and wind speed. This means that this kind of renewable energy is not a stable supply of energy and requires high wind velocities in a range of 5 to 25 m/s.

Magnus wind turbines can overcome most of existing turbines limitations used nowadays, such its low efficiency at the most repeatable wind velocities V < 7 m/s due small blade lift coefficient. Under such conditions, the power coefficient of traditional wind turbines drops rapidly to zero at about V = 4 m/s. On the other hand, the Magnus wind turbines can be exploited in a wide range of wind velocities, that is, from 2 m/s to storm winds [1-3].

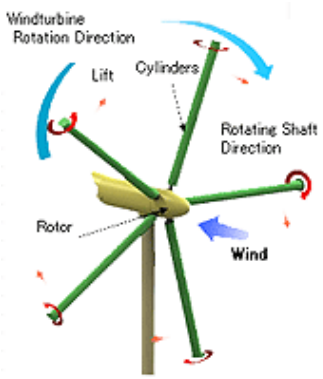

Fig. 1. Magnus wind power generator [4]

The Magnus effect is based on generation of a sidewise force on a spinning cylindrical or spherical solid immersed in a fluid when there is a relative motion between the spinning body and the fluid.

In order to obtain the Magnus force, an induced rotation, produced by an external impeller, is needed on the spinning cylinder, being the main inconvenient of this kind of turbines. The purpose of this study is to bring an attempt to generate Magnus force using a centrifugal rotor instead of external powered cylinder. Three different autorotation geometries operating under five steady-state flow fields have been designed and analysed using PIV.

Although a good number of investigations on wind wake turbine aerodynamics have been conducted in the recent years, very few experimental investigations can be found in literature to provide detailed field measurements [5].

2. Principle: Magnus effect.

A revolving body under spinning and relative translational velocity in a fluid is subjected not only to drag, but also to a lift. Fluid flow at body surroundings pass easily in the side that either the spinning and translational velocity have the same direction **Fig. 2**.

Inversely, on the other side, angular velocity of the body offers resistance to the fluid flow. Flow differences in both sides induced by spinning velocity generate, in accordance with Bernoulli's principle, a pressure gradient resulting in a net force on the body perpendicular to the flow vector.

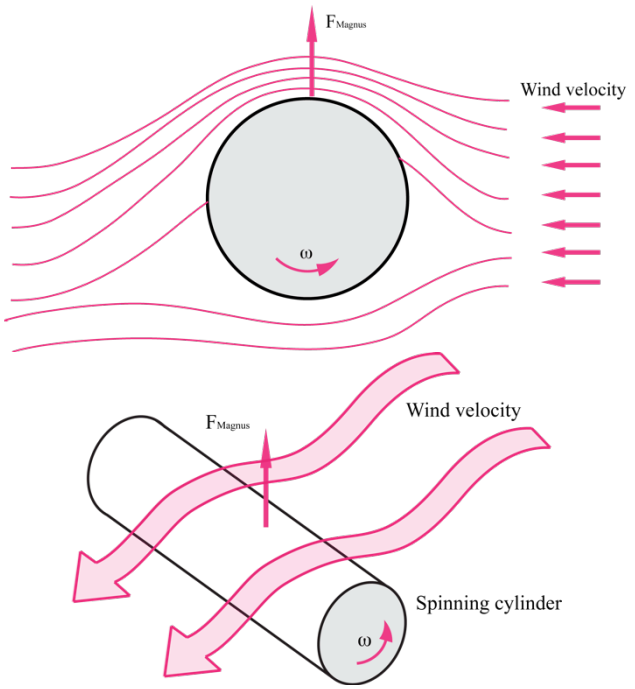

Fig. 2. Magnus effect. Lines represent the wind velocity and the arrow F_{Magnus} represents the resulting force towards the side of lower pressure.

Lift force generated over the cylinder is the responsible of the wind turbine rotation.

The aerodynamic force is the total of drag and lift force. The lift force is also called the Magnus force, named after his discoverer by German physicist Heinrich Magnus. He described the effect of force acting perpendicular to the line of motion of a spinning ball in 1852.

Magnus force over a spinning cylinder was quantified by Kutta-Joukowski theorem, and it states that the resulting force is directly dependent on the flow velocity vector v, the vortex strength or circulation Γ, cylinder length l and air density ρ.

$$F_{Mag} = \rho \Gamma v l \tag{1}$$

The vortex strength is defined as the fluid velocity υ on a small element by the differential length of this element dL.

$$\Gamma = \oint_C \upsilon \, dL = 2\pi r V \tag{2}$$

Where r is the radius of the cylinder and V is the rotational speed calculated with the following equation.

$$\boldsymbol{V} = \boldsymbol{\omega} \cdot \boldsymbol{r} \tag{3}$$

Where ω is the angular rotation of the cylinder.

3. Rotor geometries

Although the above equations are valid only if a cylinder is considered, the same principle can be observed when an autorotation rotor is used instead.

During investigation, a total of three prototypes were made, three models of centrifugal rotor were tested. They were yielding the same rotor lengths, with the different overlap and rotor-blade diameters. Cross-sectional details of each Prototype with most important geometrical parameters are presented on Fig. 3-4, and most important blade features are given in a Table 1.

Table I. – Characteristics of tested blades.

Name	Blade Length [mm]	Blade Material	Diameter [mm]	No. blades
Prototype 1	200	Al	60	#22
Prototype 2	200	Al	60	#11
Prototype 3	200	Al	60	#6

Fig 3. Geometries analysed. Prototypes 1, 2 and 3 respectively.

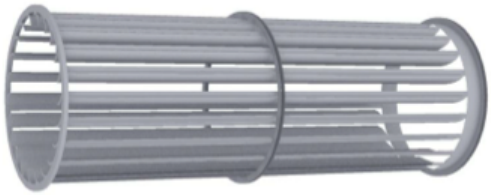

Fig 4. Prototype 1 perspective.

5. Experimental setup and facility

Experiments took place in the subsonic close-circuit wind tunnel at the GREFEMA research laboratory. Set of the operating wind velocities from 0 – 55 m/s is obtained using an axial fan powered by a variable three-phase 30 kW motor.

The airflow is controlled by changing the blower rotation from 0 – 50 Hz and monitored using an anemometer placed in the undisturbed field, right before the test section.

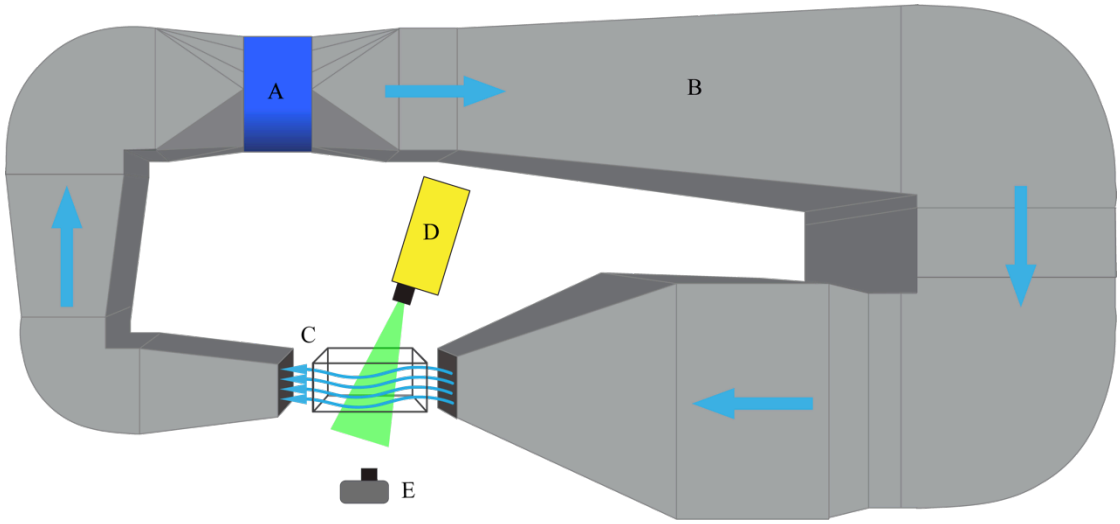

Fig. 5. GREFEMA subsonic close-circuit wind tunnel. A: Variable speed fan. B: Close-circuit conductions. C: Methacrylate box. D: Laser source. E: High speed camera. Blue arrows indicate airflow direction.

The working volume is an acrylic box of 40x40x130 cm with a maximum working wind speed of 55 m/s at the test section.

PIV system light source is a LaserPulse Nd: Yag of 532 nm, 120 mJ/pulse and 14,8 Hz. High sensibility acquisition camera of 2 Mpx is used to capture the high frequency images needed to carry out the analysis.

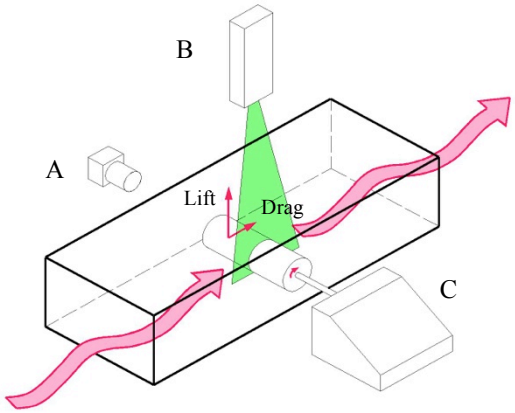

Fig 6. PIV working volume detail. A: High speed camera. B: Laser source. C: Force balance.

A force balance is used to measure the aerodynamic reaction forces and moments on the model. In this experiment it is used to measure the axial and normal force relative to the rotation sting as shown in Fig. 6. Using the axial and normal force, the lift and drag force can be obtained. Since the lift and the drag forces that act upon the rotor as the rotational cylinder are function of the angular velocity of the cylinder itself, measurement of the rotor angular velocity is necessary. Then, a tachometer is used for the spinning measurements.

After the rotor is positioned at the desired location, the rotation of the Magnus wheel is set to still condition and the measurement takes place after some settling period of time, so constant rotational speed of the cylinder can be reached. This procedure is repeated for various wind speeds, for all the blades and for the every prototype tested.

6. Results and discussion

Regardless of the fact that some of the prototypes operate satisfactory for high wind speeds and some showed good cut-in characteristic, angular velocities of 5, 10, 15 and 25 m/s are chosen.

In order to understand and assess various models, a rotation results for all prototypes are compared and presented on Fig. 8 in rpm values. On Fig. 9, tip speed ratios of the tested prototypes are shown as a function of the wind speed. Tip speed ratio of the rotor is defined as follows,

$$\lambda = \frac{\frac{D}{2}\cdot 2\pi\cdot\frac{n_{rotor}}{60}}{U_{wind}} = \frac{R_s\cdot\omega_{rotor}}{U_{wind}} \quad (4)$$

where λ is the TSR of the rotor, R_s is the rotor's radius, ω_{rotor} is the angular velocity and U_{wind} is the wind speed.

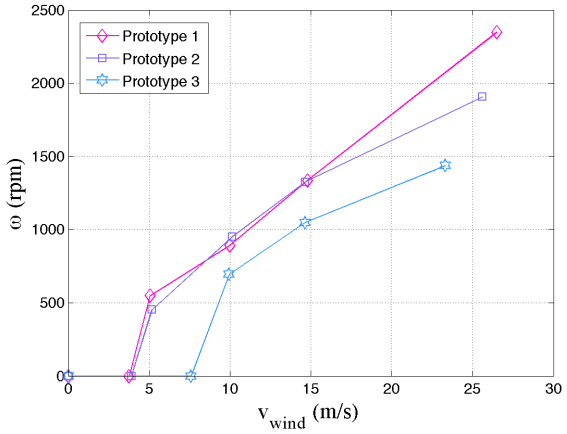

Fig 7. Angular velocity of tested prototypes.

Fig. 7 shows that as the wind speed increases, the angular rotation also increases. It could be observed that high number of blades produces high angular speeds but no significant differences between prototypes 1 and 2. One of the noticeable advantages of the prototypes 1 and 2 is the low cut-in speed needed to start the rotation.

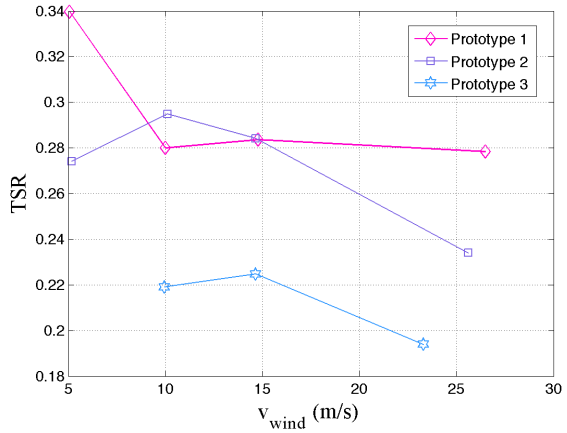

Fig 8. Tip speed ratio of tested prototypes.

In Fig. 8, the values of tip speed ratios are extremely low due to small prototype radius. The 22-blade rotor has higher TSR values.

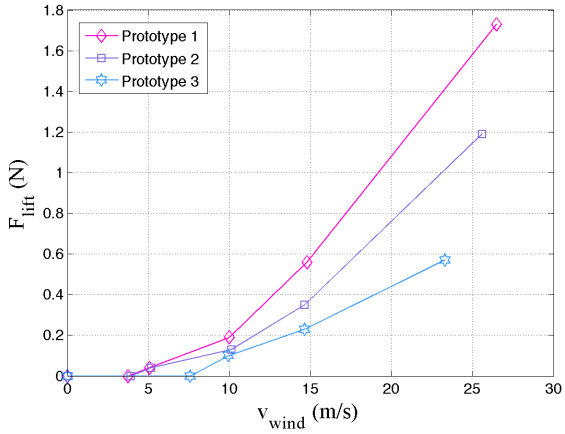

Fig 9. Lift force of tested prototypes.

The wind speed dependence of the steady state lift force is shown in Fig. 9. As expected, the lift force increases as the wind speed grows. It also can be observed that lift force is directly dependant to blade number. It means that larger dragging surface produce much more pressure difference between rotor faces.

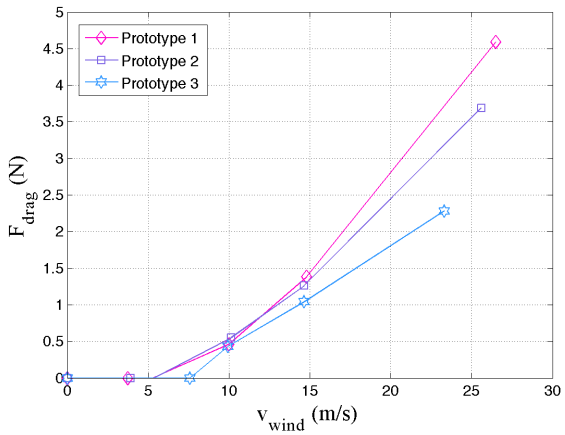

Fig 10. Drag force of tested prototypes.

As happens with the lift force, drag force also increases with the speed velocity, Fig. 10. It also can be corroborated that the more working surface the prototype has, the more drag force obtained.

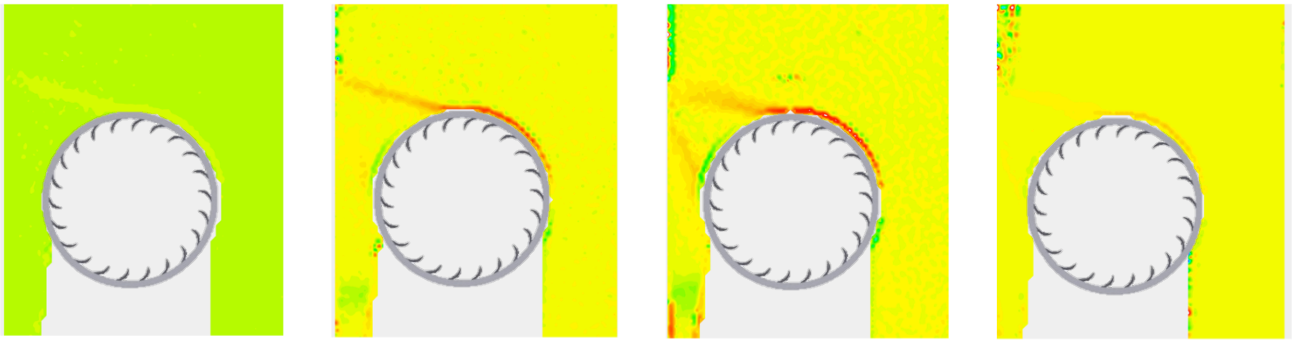

Fig. 11. Propagation of the tip vortices in prototype 1.

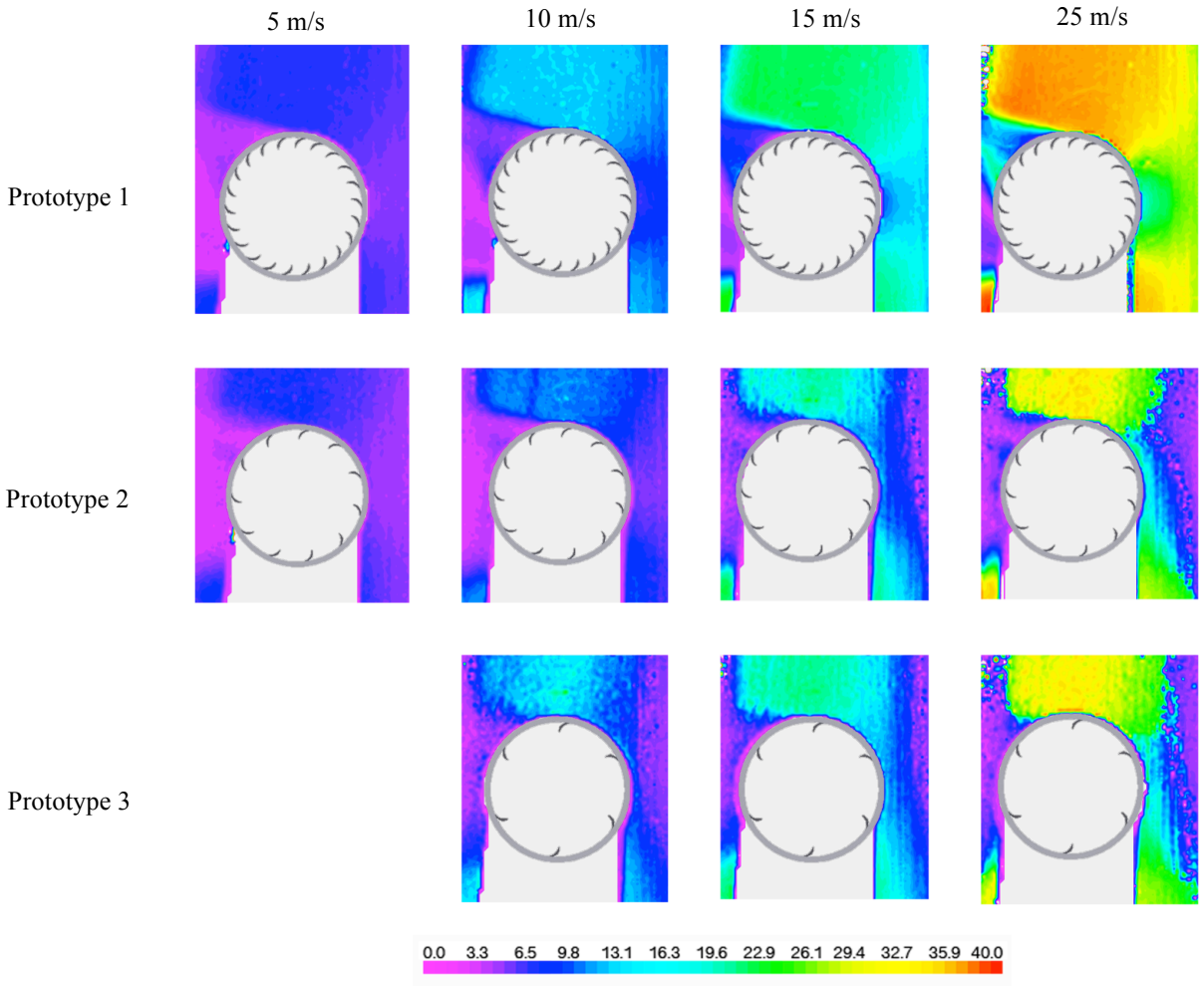

Fig. 12. Cross sectional air velocity profile around the rotor. Units in m/s.

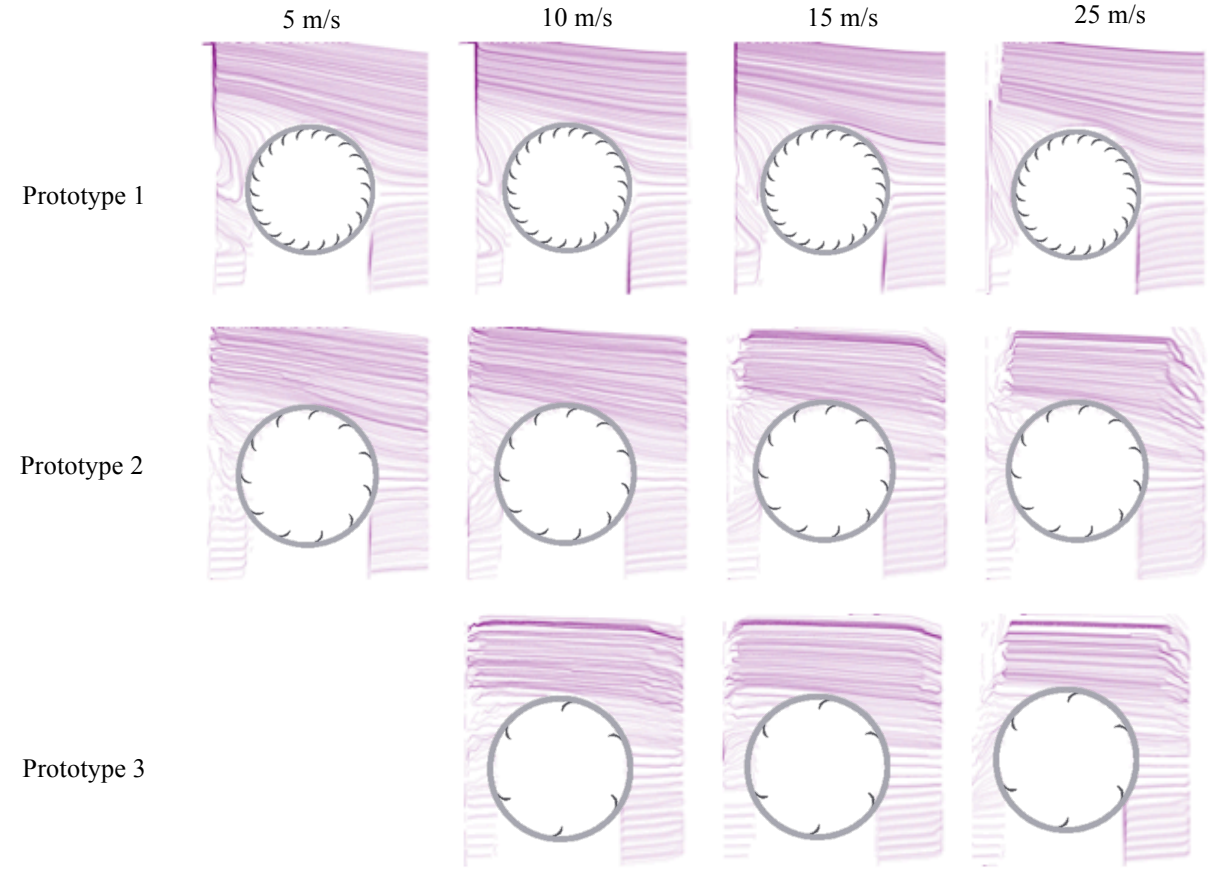

Fig. 13. Horitzontal stream lines that formed around the rotor.

PIV is also used to identify the mean vorticity field while the blades were rotating. Fig. 11 clearly reveals the presence of punctual vortices, which form at the blade tip and along the superior rotor boundary layer. The colours are arbitrarily chosen and provide clarity in understanding the path of vortices generated by each blade.

Finally, airflow patterns around the rotor are presented in Fig. 12 and Fig. 13. As the flow approaches the rotor the streamlines separate, moving either up or down to flow around the cylinder. Notice that the distance between the streamlines changes. In front of and behind the cylinder the streamlines are further apart; above and below the cylinder they are closer together. In case of prototype 3, it is clearly shown, where streamlines trajectory is not modified and completely horizontal whatever the wind velocity is.

The vortex caused by the cylinder's rotation will add to the velocity of the flow above the rotor, and subtract from the velocity of the flow beneath the rotor. Notice also that the circulatory flow has induced upwash ahead of the cylinder and downwash behind it.

The air flowing above the rotor is flowing faster than the air flowing below the rotor. Consequently the static pressure above the cylinder is lower than the static pressure below the cylinder. This results in an unbalanced force giving a net upwards aerodynamic force.

The combination of this net upwards force with the net horizontal force caused by drag, produces a total reaction which is inclined rearwards with respect to the free stream flow, called the Magnus effect.

7. Conclusions

The effect of blade number has been evaluated using a subsonic wind tunnel equipped with a particle image velocimetry system and a force balance. Results indicate that a major number of blades cause a higher rotation and, consequently, a stronger lift force.

In addition, with higher wind velocities, vorticity field on the upper rotor part decreases, which means that airflow penetrates better in it.

Although the Magnus force obtained take values lower than 1,8 N, it's important to highlight that this force is obtained freely harvesting the wind energy and taking into account that the size of the rotor tested is four times smaller than a theoretical smooth one.

Moreover, finished the experimental tests we can confirm the small noise levels produced by this kind of turbine.

Further work will focus on obtaining higher TSR values, using rotors with higher blades surfaces, larger radius or making use of deflectors to guide the airflow tangentially to the blades.

Regardless of the experimental analysis of the centrifugal Magnus wind turbine, current research leaves open space for the possible model improvements and further investigations.

Model improvement could include solution for problems such as an overstress of the shaft for wind speeds higher then 20 m/s and possible substitution of the materials or support structure in order to avoid the resonance due the low natural frequencies of the blades. Other solutions should be investigated as well, together with the possibility of bigger prototype investigations.

References

[1] Goňo, Radomír, Rusek, Stanislav, Hrabčík, Miroslav, Wind turbine cylinders with spiral fins.

[2] C. A. Pomeroy, "Revolutionary Spiral Fin Turbine," in The Japan Journal, August 2008 Vol. 5 No. 4.

[3] MECARO Co. Ltd., company documentation.

[4] Nobuhiro Murakami, Akita, US 2007/0046029 A1, Magnus type wind power generator.

[5] Kozlov, V. and Bychkov, N., Magnus Wind Turbine, Experimental Results of the Model Testing, Institute of Theoretical and Applied Mechanics SB RAS, 2005.